© 2017. Published by The Company of Biologists Ltd | Development (2017) 144, 4015-4025 doi:10.1242/dev.151746

RESEARCH ARTICLE

Nuclear movement regulated by non-Smad Nodal signaling via JNK is associated with Smad signaling during zebrafish endoderm specification

Shunya Hozumi, Shun Aoki and Yutaka Kikuchi*

ABSTRACT

Asymmetric nuclear positioning is observed during animal development, but its regulation and significance in cell differentiation remain poorly understood. Using zebrafish blastulae, we provide evidence that nuclear movement towards the yolk syncytial layer, which comprises extraembryonic tissue, occurs in the first cells fated to differentiate into the endoderm. Nodal signaling is essential for nuclear movement, whereas nuclear envelope proteins are involved in movement through microtubule formation. Positioning of the microtubule-organizing center, which is proposed to be crucial for nuclear movement, is regulated by Nodal signaling and nuclear envelope proteins. The non-Smad JNK signaling pathway, which is downstream of Nodal signaling, regulates nuclear movement independently of the Smad pathway, and this nuclear movement is associated with Smad signal transduction toward the nucleus. Our study provides insight into the function of nuclear movement in Smad signaling toward the nucleus, and could be applied to the control of TGFβ signaling.

KEY WORDS: Nuclear movement, Endoderm specification, Nodal, Smad, JNK, MTOC

INTRODUCTION

The largest organelle, the nucleus, is not always located in the center of the cell. Asymmetrical positioning of the nucleus has been observed in differentiated animal cells and tissues, including skeletal muscle, many epithelial cells, and neurons (Dupin and Etienne-Manneville, 2011; Gundersen and Worman, 2013). Abnormal positioning leads to cellular dysfunction and diseases, such as muscular dystrophy, cardiomyopathy and lissencephaly (Gundersen and Worman, 2013; Bone and Starr, 2016). The positioning of the nucleus is dynamically regulated during cell division and migration (Dupin and Etienne-Manneville, 2011; Gundersen and Worman, 2013). Recent studies revealed that nuclear positioning is controlled by microtubules (MTs), actins, and associated motor proteins. In addition, the linker of nucleoskeleton and cytoskeleton (LINC) complex, which is composed of outer nuclear membrane KASH-domain (Klarsicht, ANC-1 and Syne homology) proteins and inner nuclear membrane SUN-domain (Sad1p and UNC-84) proteins (Bone and Starr, 2016; Dupin and Etienne-Manneville, 2011; Gundersen and Worman, 2013), has been shown to be involved in nuclear positioning. It has been suggested that the position of the microtubule-organizing center (MTOC) and the connection between the MTOC and the nucleus are crucial for MT-mediated nuclear movement (Bone and Starr, 2016; Gundersen and Worman, 2013).

Although many studies have suggested that nuclear positioning plays an important role in cellular function, only one study has reported on the relationship between nuclear positioning, asymmetric signaling, and cell fate determination (Del Bene et al., 2008; Gundersen and Worman, 2013). In the developing zebrafish retina neuroepithelium, nuclear movement, termed interkinetic nuclear migration, is correlated with cell cycle exit and Notch signaling activation; this process is regulated by Syne (a LINC complex protein) and the motor protein Dynactin 1 (Del Bene et al., 2008; Gundersen and Worman, 2013). However, the exact mechanisms of nuclear movement, and the relationship between nuclear movement and cell fate determination, remain to be elucidated.

Nodal, a transforming growth factor β (TGFβ) superfamily member, is a ligand that regulates the expression of its target genes by binding to serine/threonine kinase receptors and inducing the phosphorylation of Smad2/3 (Di Guglielmo et al., 2003; Penheiter et al., 2002; Hayes et al., 2002). In mouse and zebrafish embryos, Nodal is essential for mesendoderm induction prior to gastrulation (Weinstein et al., 1998; Nomura and Li, 1998; Jia et al., 2008). Genetic analyses in zebrafish revealed that two *Nodal*-related genes, *nodal-related 1* (*ndr1*) and *ndr2*, are essential, and that the EGF-CFC family gene *teratocarcinoma-derived growth factor 1* (*tdgf1*), which encodes a co-receptor of Nodal, is necessary for mesendoderm induction (Schier, 2009). In addition, analyses using various zebrafish mutants and knockdown experiments have identified molecular pathways leading to the endoderm cell fate (Fukuda and Kikuchi, 2005; Zorn and Wells, 2009). It has been shown that Sox32 (Casanova) is an essential transcription factor for endoderm fate determination downstream of Nodal/Smad signaling (Dickmeis et al., 2001; Kikuchi et al., 2001). Aside from the Smad pathway, TGFβ also activates non-Smad signaling pathways, such as extracellular signal-regulated kinase (Erk), p38 (Mapk14) and c-Jun N-terminal kinase (JNK) (Moustakas and Heldin, 2005; Derynck and Zhang, 2003; Mu et al., 2012). Smad and non-Smad signaling pathways are involved in the regulation of various cellular processes, including cell differentiation, proliferation, migration and epithelial-mesenchymal transition (EMT) through cell context-dependent transcription and the regulation of cytoskeleton and cell junction formation (Moustakas and Heldin, 2005; Derynck and Zhang, 2003; Mu et al., 2012); however, the interactions between these pathways are poorly understood.

During the course of our analysis of endoderm specification, we discovered distinct nuclear movement toward the yolk syncytial layer (YSL) in the most laterally located marginal cells (lateral

Department of Biological Science, Graduate School of Science, Hiroshima University, Kagamiyama 1-3-1, Higashi-Hiroshima, Hiroshima, 739-8526 Japan.

*Author for correspondence (yutaka@hiroshima-u.ac.jp)

Y.K., 0000-0001-5688-7358

Received 9 March 2017; Accepted 14 September 2017

Development (2017) 144, 4015-4025 doi:10.1242/dev.151746

marginal cells, or LMCs), which are the first cells fated to differentiate into the endoderm. In this study, we explored the regulation and significance of nuclear movement in LMCs by Nodal signaling, and identified that the non-Smad JNK signaling pathway regulates nuclear movement independently of Smad; this movement leads to transduction of the Smad signal toward the nucleus.

RESULTS

Nodal signaling is necessary for nuclear movement toward the YSL in the most laterally located marginal cells during endoderm specification

In order to explore the process of endodermal fate determination from the sphere [4.0 h post fertilization (hpf)] to the late blastula stage (4.7 hpf), we carefully observed the spatiotemporal emergence and distribution of *sox32*-expressing endoderm cells in the marginal domain of wild-type (WT) embryos using fluorescence *in situ* hybridization (FISH). Expression of *sox32* was first detected in LMCs located adjacent to both the YSL and the enveloping layer (EVL) cells (Fig. 1A, green cell). At 4.7 hpf, 97.7% (43/44) of LMCs were *sox32*$^{+}$ (Fig. 1B,B′, arrowheads). By contrast, medial marginal cells (MMCs) (Fig. 1A, red cells), which were adjacent to both LMCs and the YSL, did not express *sox32* at 4.7 hpf [2.3% (1/44) of MMCs were *sox32*$^{+}$; Fig. 1B,B′, arrows], indicating that LMCs are the first endoderm specified cells in zebrafish embryos.

Nuclear positioning of LMCs in WT embryos at 4.7 hpf appeared to be closer to the YSL as compared with that at 4.0 hpf (Fig. 1B,B′, D, arrowheads). In addition, nuclear positioning of LMCs appeared to be more distant from the YSL following treatment with the TGFβ type I receptor inhibitors SB505124 or SB431542 (Laping et al., 2002; Inman et al., 2002; Callahan et al., 2002; DaCosta Byfield et al., 2004), at 4.7 hpf (Fig. 1E,F, arrowheads). This suggests that Nodal signaling is involved in determination of nuclear positioning in LMCs. Confocal time-lapse analysis clearly showed that while the nuclei in both LMCs and MMCs moved toward the YSL, those in LMCs were closer to the YSL than those in MMCs between 4.0 and 4.7 hpf (Movies 1 and 2).

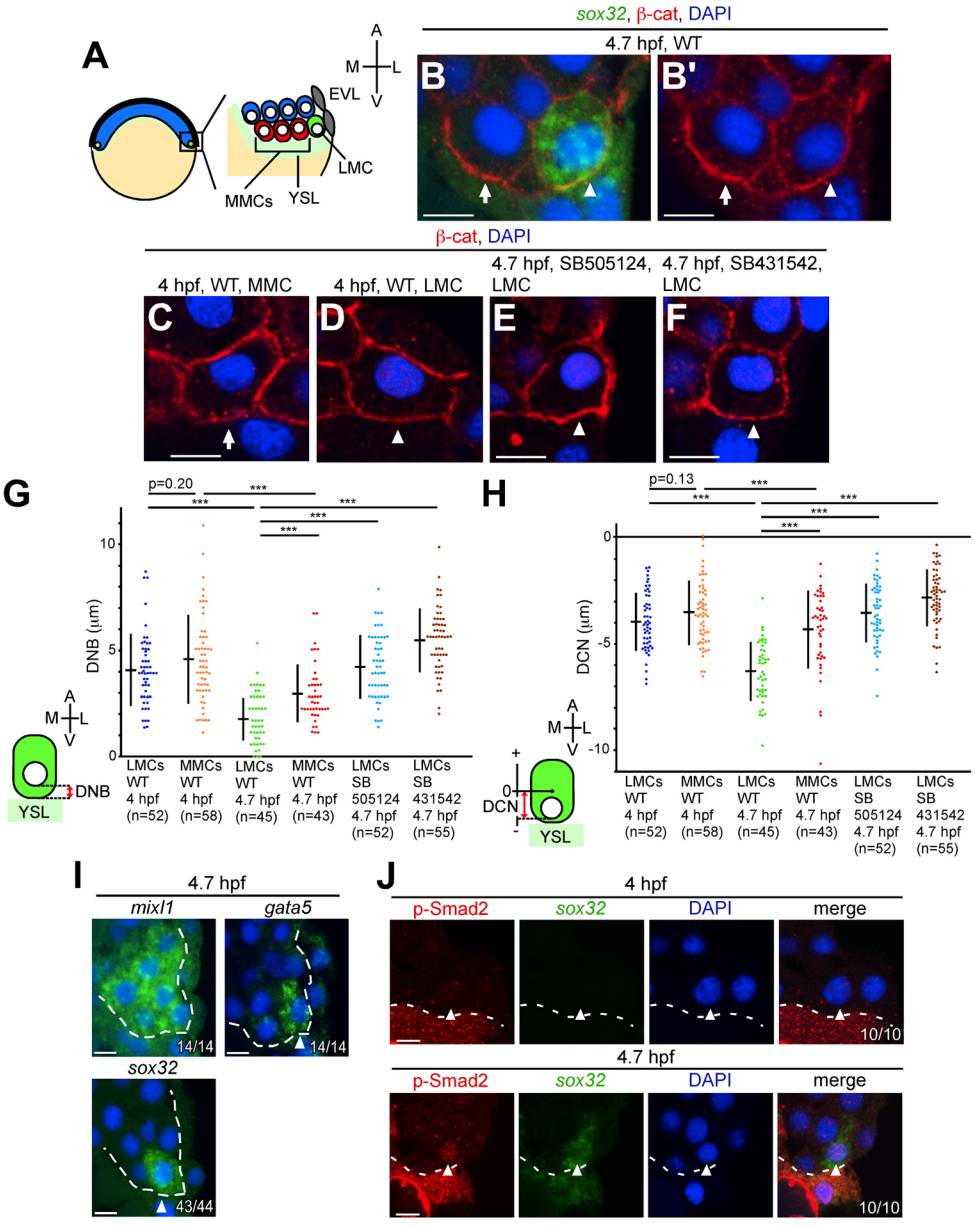

Fig. 1. Nuclear movement toward the YSL in LMCs occurs at 4.7 hpf. (A) Illustration of the zebrafish blastula embryo (left) and location of marginal cells (right). LMCs refers to the most laterally located marginal cells (green); MMCs, medial marginal cells (red); EVL, enveloping layer; YSL, yolk syncytial layer; A, animal; V, vegetal; M, medial; L, lateral. (B-F) Transverse sections of wild-type (WT) and TGFβ type I receptor inhibitor (SB505124 or SB431542)-treated embryos. The cell membrane and the nucleus are visualized by β-catenin (β-cat) and DAPI staining, respectively. The endoderm marker *sox32* was detected by FISH (B only). Arrows and arrowheads indicate MMCs and LMCs, respectively. (G) Minimum distance between the most vegetal position of the nucleus and the blastoderm/YSL boundary (DNB) in WT and TGFβ receptor inhibitor-treated embryos. (H) Minimum distance between the center of the cell and the most vegetal position of the nucleus (DCN) relative to the animal-vegetal axis in WT and TGFβ receptor inhibitor-treated embryos. In the DCN, the center of the cell is defined as zero; the animal and vegetal sides relative to the center of cell are set as plus and minus along the animal and vegetal axes, respectively. (G,H) ***P<0.001. n, number of nuclei examined. (I) Transverse sections of WT embryos showing *mixl1*, *gata5* and *sox32* FISH (green) at 4.7 hpf. DAPI, blue. The number of embryos showing this pattern among the total examined is indicated bottom right. Arrowheads indicate LMCs. Dashed lines indicate the boundary between the blastoderm and the YSL or EVL. (J) Transverse sections of WT embryos; p-Smad2 and *sox32* were visualized via immunohistochemical staining and FISH, respectively. Arrowheads indicate the nucleus in LMCs. Dashed lines indicate the boundary between the blastoderm and the YSL. Scale bars: 10 μm.

Development (2017) 144, 4015-4025 doi:10.1242/dev.151746

In order to evaluate nuclear movements during endoderm specification, we measured the minimum distance between the most vegetal position of the nucleus and the blastoderm/YSL boundary (distance nucleus to blastoderm, or DNB) (Fig. 1G). The mean DNB value in LMCs of WT embryos was significantly reduced from 4.10 µm at 4.0 hpf to 1.75 µm at 4.7 hpf; this reduction was blocked by treatment with SB505124 or SB431542 (Fig. 1G). We also investigated the positional change of nuclei in MMCs (Fig. 1A) at 4.7 hpf. The mean DNB value in MMCs at 4.7 hpf was slightly, but significantly, lower than that at 4.0 hpf, and at 4.7 hpf the mean DNB value in LMCs was significantly lower than that in MMCs (Fig. 1G). We also explored the minimum distance between the center of the cell and the most vegetal position of the nucleus (distance center to nucleus, or DCN) (Fig. 1H). We did not detect any marked differences between DNB and DCN values in the positional change of nuclei in LMCs and MMCs (Fig. 1G,H). We next examined the nuclear positioning of LMCs and MMCs relative to the center of the cells (Fig. S1). The results indicated that 57% of nuclei in LMCs at 4.0 hpf are localized between zero and approximately +90°. At 4.7 hpf, 67% of LMCs had shifted to between zero and approximately −90° (Fig. S1). More than 50% of the nuclei in MMCs of WT embryos and in LMCs of SB505124-treated or SB431542-treated embryos maintained their positions at 4.7 hpf (Fig. S1). These results showed that the nuclei of LMCs in WT embryos move toward the YSL between 4.0 and 4.7 hpf and that Nodal signaling is necessary for this nuclear movement.

We and others have previously shown that both Mixl1 and Gata5 are necessary for endoderm specification downstream of Nodal signaling and upstream of Sox32 (Fukuda and Kikuchi, 2005; Zorn and Wells, 2009). We examined *mixl1* and *gata5* expression at 4.7 hpf, and found that *mixl1* is widely expressed in marginal cells, whereas *gata5* expression is restricted to the LMCs (Fig. 1I). Consistent with previous results, *sox32* expression was only detected in LMCs, along with *mixl1* and *gata5* (Fig. 1I). In addition, at late blastula stage, expression of *gata5* was restricted to the mesendoderm, which is a region comprising three to four rows of cells from the margin (Alexander et al., 1999; Rodaway et al., 1999; Ober et al., 2003), suggesting that high Nodal signaling is necessary for *gata5* expression. To confirm that Nodal signaling is highly activated only in the nucleus of LMCs at 4.7 hpf, we used an antibody for phosphorylated Smad2 (p-Smad2), a downstream effector of Nodal signaling. A previous report showed that the overexpression of Smad2/3 containing mutated phosphorylation sites repressed mesendoderm induction in zebrafish embryos (Jia et al., 2008), suggesting that p-Smad2 plays a significant role in endoderm specification. Both p-Smad2 protein and *sox32* mRNA were detected only in the nuclei of LMCs at 4.7 hpf, and not at 4.0 hpf (Fig. 1J). These results indicate that p-Smad2 nuclear translocation, which leads to *sox32* induction, is associated with nuclear movement toward the YSL in LMCs.

Enhancement of Nodal signaling in the YSL induces nuclear movement in MMCs toward the YSL

Having shown that nuclear movement of LMCs requires Nodal signaling during endoderm specification, we then wanted to confirm whether Nodal overexpression induces nuclear movement in MMCs toward the YSL. *ndr1* mRNA, together with dextran-Alexa Fluor 594, was injected into the YSL at 3.0 hpf (Fig. 2A). Fluorescence was only observed in the YSL due to the lack of permeability between the blastoderm and the YSL (Fig. 2C,C′, brackets), consistent with previous results (Gritsman et al., 1999). Mean DNB and DCN values in MMCs of WT embryos were reduced from 3.30 µm to 1.12 µm and from −4.53 µm to −5.45 µm, respectively, at 4.7 hpf, when *ndr1* mRNA was overexpressed in the YSL (*ndr1* mRNA>YSL) (Fig. 2B-E). In addition, nuclear positioning in MMCs was between zero and approximately +90° (48%) in WT embryos (Fig. 2F), whereas 76% of nuclei in MMCs were located between zero and approximately −90° in *ndr1* mRNA>YSL embryos (Fig. 2F), similar to what was observed for the nuclei of LMCs at 4.7 hpf (Fig. S1). Therefore,

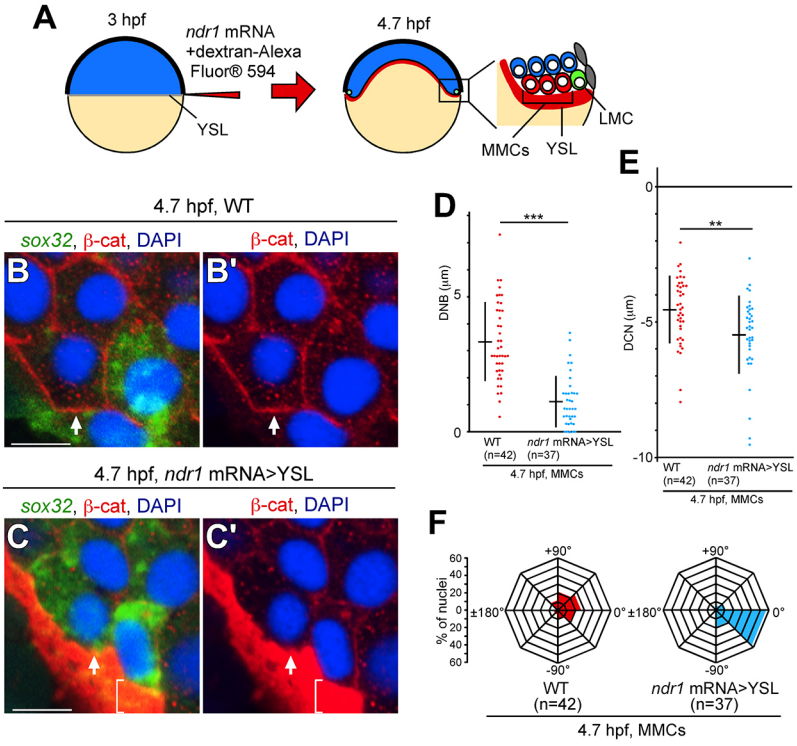

Fig. 2. Overexpression of *ndr1* mRNA in the YSL leads to nuclear movement in MMCs toward the YSL.
(A) Experimental design for *ndr1* mRNA overexpression in YSL (*ndr1* mRNA>YSL). (B-C′) Transverse sections of WT and *ndr1* mRNA>YSL embryos; the cell membrane, nucleus and *sox32* mRNA were visualized by β-cat staining, DAPI staining and FISH, respectively at 4.7 hpf. Arrows indicate MMCs. Brackets indicate the fluorescence of dextran-Alexa Fluor 594 in the YSL. Both nuclear movement and *sox32* expression in MMCs were induced by *ndr1* mRNA>YSL at 4.7 hpf. Scale bars: 10 µm. (D,E) DNB and DCN in MMCs were measured in WT and *ndr1* mRNA>YSL embryos. ***P<0.001, **P<0.05. (F) Angles between the center of the cell and the nucleus relative to the medial-lateral axis were measured in WT and *ndr1* mRNA>YSL embryos as shown in Fig. S1. *n*, number of nuclei examined (D-F).

Development (2017) 144, 4015-4025 doi:10.1242/dev.151746

Nodal signaling has the ability to induce nuclear movement not only in LMCs, but also in MMCs.

Functional inhibition of LINC complex proteins blocks nuclear movement in LMCs, probably through MTOC attachment to the nucleus and MT formation

Previous reports indicated that the KASH domain, a component of LINC complex proteins, is required for nuclear migration in *Drosophila* and *C. elegans* (Bone and Starr, 2016; Dupin and Etienne-Manneville, 2011; Gundersen and Worman, 2013). Overexpression experiments using a KASH domain of Syne2a (C-Syne2a), which functions as a dominant-negative form of this protein, showed that positioning of cell nuclei in zebrafish photoreceptors is dependent on the Syne gene family (Tsujikawa et al., 2007). These results prompted us to analyze the function of LINC complex proteins in endoderm specification and nuclear movement of LMCs using C-Syne2a (Tsujikawa et al., 2007).

We first monitored the effect of *C-syne2a* mRNA overexpression on endoderm specification using the endoderm marker *sox32*. Whole-mount *in situ* hybridization (WISH) and quantitative PCR (qPCR) analyses indicated that expression of both *sox32* and the mesodermal marker *T, brachyury homolog a* (*ta*) was significantly reduced in *C-syne2a*-overexpressing embryos compared with that in nuclear *lacZ* (*nlacZ*)-overexpressing embryos at 5.3 hpf, without affecting the expression of *ndr1* and *ndr2* (Fig. S2). The mean DNB and DCN values of LMCs in WT embryos were 2.13 µm and −5.93 µm, respectively, at 4.7 hpf, whereas those of *C-syne2a*-overexpressing embryos were 4.24 µm and −3.51 µm (Fig. 3A-D). At 4.7 hpf, 58% of nuclei in LMCs of *C-syne2a*-overexpressing embryos were localized between zero and +90° (Fig. 3E), similar to observations of LMC nuclei at 4.0 hpf (Fig. S1). Therefore, overexpression of *C-syne2a* resulted in the inhibition of nuclear movement toward the YSL in LMCs. In addition, whereas *sox32*-expressing nuclei in LMCs were p-Smad2^{+} in WT embryos, *sox32* was not expressed and p-Smad2 was absent in LMCs of *C-syne2a*-overexpressing embryos at 4.7 hpf (Fig. 3F). These results suggest that LINC complex proteins regulate both nuclear movement and p-Smad2 nuclear translocation in LMCs to induce endoderm specification.

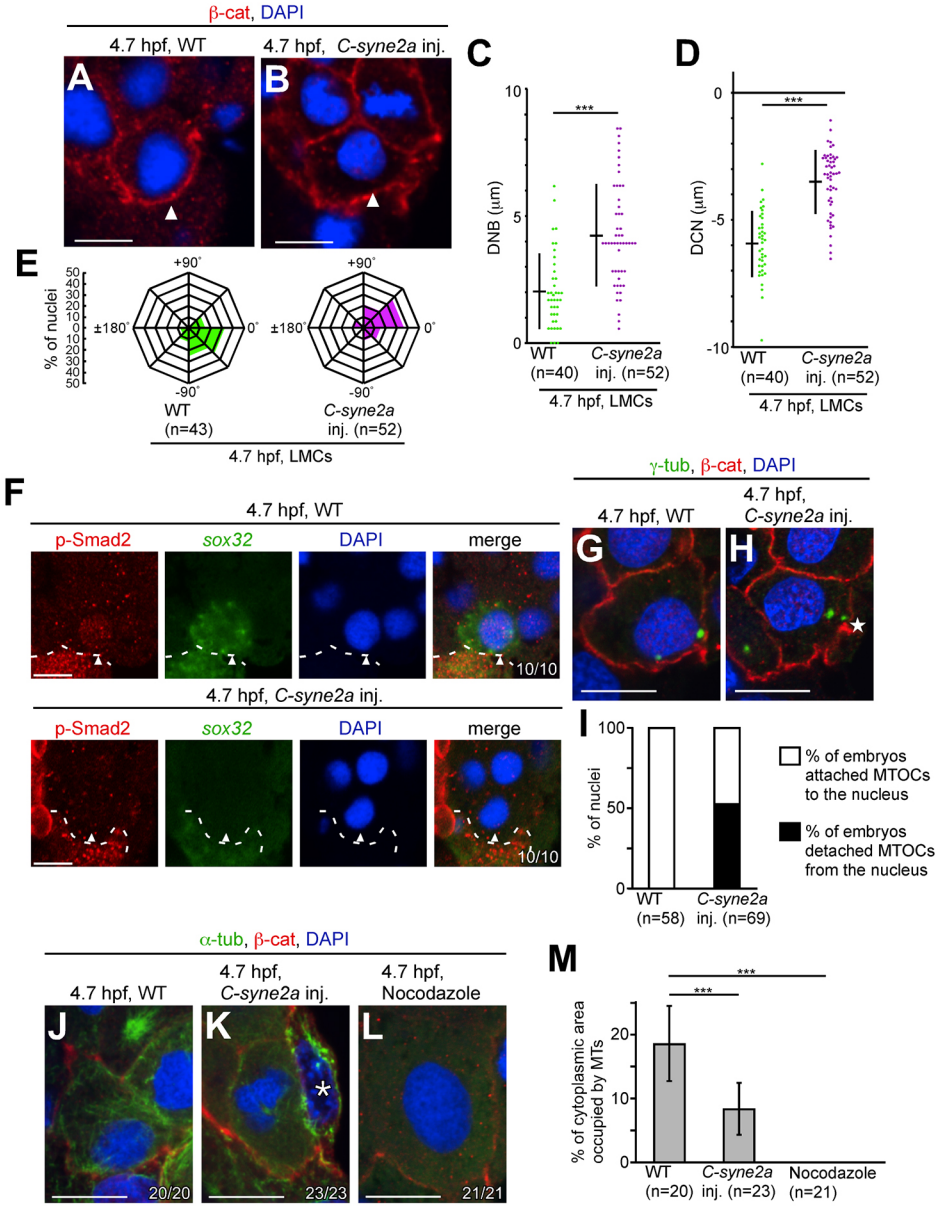

Fig. 3. *C-syne2a* overexpression prevents nuclear movement and p-Smad2 nuclear translocation in LMCs, possibly through regulation of MTOC positioning and MT formation. (A,B) Nuclear positioning in LMCs in WT and *C-syne2a*-overexpressing embryos at 4.7 hpf. Transverse sections of WT and *C-syne2a*-overexpressing embryos; cell membrane and nucleus were visualized by β-cat and DAPI staining, respectively. Arrowheads indicate LMCs. (C,D) DNB and DCN in LMCs were measured in WT and *C-syne2a*-overexpressing embryos at 4.7 hpf. *n*, number of nuclei examined. ***P<0.001. (E) Angles between the center of the cell and the nucleus in LMCs relative to the medial-lateral axis were measured as shown in Fig. S1. *n*, number of nuclei examined. (F) Transverse sections of WT embryos; p-Smad2 and *sox32* were visualized by immunohistochemical staining and FISH, respectively. The number of nuclei examined is shown bottom right. Arrowheads indicate nuclei in LMCs. Dashed lines indicate the boundary between the blastoderm and the YSL. (G,H) Transverse sections of WT and *C-syne2a*-overexpressing embryos; cell membrane and MTOCs were visualized by β-cat and γ-tubulin (γ-tub) staining, respectively at 4.7 hpf. The star (H) indicates an MTOC that has detached from the nucleus in *C-syne2a*-overexpressing embryos. (I) Percentage of embryos with attached or detached MTOCs in WT or *C-syne2a*-overexpressing embryos at 4.7 hpf. *n*, number of nuclei examined. (J-L) Transverse sections of WT, *C-syne2a*-overexpressing and nocodazole-treated embryos; cell membrane, MTs and nuclei were visualized by β-cat, α-tub and DAPI staining, respectively at 4.7 hpf. The number of embryos examined is shown bottom right. An asterisk (K) indicates the EVL cell. (M) Percentage of cytoplasmic area occupied by MTs in LMCs of WT, *C-syne2a*-overexpressing and nocodazole-treated embryos. *n*, number of embryos examined. Error bars indicate s.d. of 20, 23 or 21 measurements. ***P<0.001. Scale bars: 10 µm.

Development (2017) 144, 4015-4025 doi:10.1242/dev.151746

LINC complex proteins are known to mediate the connection between the nuclear envelope and components of the cytoskeleton (MTs and actin filaments)/MTOCs (Bone and Starr, 2016; Gundersen and Worman, 2013). It has been shown that nuclear attachment to MTOCs is required for pronuclear migration in *C. elegans* zygotes and for nuclear migration in *Drosophila* photoreceptor cells (Bone and Starr, 2016; Gundersen and Worman, 2013). Based on these previous results, we examined the positioning and formation of MTOCs and MTs in *C-syne2a*-overexpressing embryos. In WT embryos, two MTOCs were attached to the nucleus at 4.7 hpf, whereas the MTOCs in ∼50% of *C-syne2a*-overexpressing embryos were detached from the nucleus (Fig. 3G-I). Furthermore, MT formation in LMCs of *C-syne2a*-overexpressing embryos was significantly reduced, although higher than that of nocodazole-treated embryos (Fig. 3J-M). This might be due to the abnormal positioning of MTOCs. Our results suggest that attachment of MTOCs to the nucleus is crucial for nuclear movement via MT formation in LMCs.

Nuclear movement and MTOC positioning are regulated by the Nodal/JNK signaling pathway

C-syne2a-overexpression experiments suggested that the positioning of MTOCs and MT formation are involved in the nuclear movement of LMCs during endoderm specification. In order to evaluate the positioning of MTOCs during endoderm specification, we calculated the following parameters (Fig. 4A): the minimum distance between the most vegetal position of MTOCs and the blastoderm/YSL boundary (a); the length of the LMCs (b). The a/b ratio was significantly reduced from 0.36 at 4.0 hpf to 0.23 at 4.7 hpf, whereas treatment with TGFβ inhibitor (SB505124 or SB431542) prevented this change in the ratio between 4.0 and 4.7 hpf (Fig. 4B-E,H). These results showed that MTOCs are reoriented to a position closer to the YSL during endoderm specification, and that Nodal signaling regulates this process.

Various chemical inhibitors that block downstream signaling pathways of TGFβ were used to determine the regulatory mechanisms of MTOC reorientation by Nodal signaling. Specific inhibitors included the Rac1 inhibitor NSC23766 (Gao et al., 2004), Rock inhibitor Y 27632 (Han et al., 2001), Cdc42 inhibitor ML141, phosphoinositide 3-kinase inhibitor LY294002 (Vlahos et al., 1994), p38 MAP kinase inhibitor SB203580 (Cuenda et al., 1995), NF-κB activation inhibitor (Tobe et al., 2003) and the JNK inhibitors SP600125 (Bennett et al., 2001) and EMD 420123. WISH and qPCR showed that the expression of both *sox32* and *ta* was significantly downregulated by JNK inhibitor (SP600125) at 4.7 hpf without affecting the expression of *ndr1* and *ndr2* (Fig. S3).

We next examined MTOC reorientation, nuclear movement, MT formation, and nuclear translocation of p-Smad2 in JNK signaling-inhibited embryos. Both MTOC reorientation and nuclear movement were significantly inhibited by the two JNK inhibitors used (SP600125 and EMD 420123), when assessed at 4.7 hpf (Fig. 4F-H, Fig. 5A-E). Unlike the *C-syne2a*-overexpressing embryos, MT formation was not affected by treatment with either SB505124 or SP600125 at 4.7 hpf (Fig. S4). In addition, nuclear translocation of p-Smad2 was not detected in LMCs when JNK signaling was inhibited (Fig. 5F). We further observed the presence of phosphorylated JNK (p-JNK), an activated form, in the LMC/YSL boundary at 4.7 hpf (Fig. 6). The p-JNK signals in the boundary were significantly reduced in SB505124-treated embryos at 4.7 hpf (Fig. 6). These results suggest that MTOC reorientation, nuclear movement, and nuclear translocation of p-Smad2, all of which induce endoderm specification in LMCs, are regulated by JNK signaling downstream of Nodal in YSL.

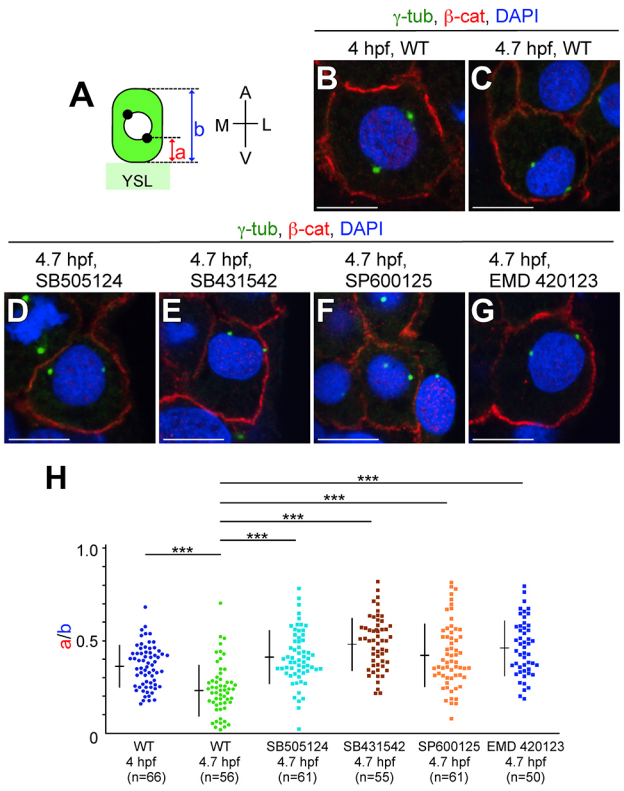

Fig. 4. MTOC reorientation in LMCs is regulated by Nodal/JNK signaling. (A) Illustration of MTOC positioning (black dots) in LMCs. a, the minimum distance between the most vegetal position of MTOCs and the blastoderm/YSL boundary; b, length of the LMC. (B-G) Transverse sections of WT and of embryos treated with SB505124, SB431542, SP600125 or EMD 420123. MTOCs, cell membrane and nuclei are visualized by γ-tub, β-cat and DAPI staining, respectively at 4.0 and/or 4.7 hpf. Scale bars: 10 µm. (H) a/b ratio in WT and inhibitor-treated embryos at 4.0 or 4.7 hpf. *n*, number of nuclei examined. ***P<0.001.

Non-Smad JNK signaling regulates nuclear movement independently of the Smad2 pathway

It is well known that Smad and non-Smad pathways, including JNK signaling, are downstream of TGFβ (Derynck and Zhang, 2003; Moustakas and Heldin, 2005; Mu et al., 2012). We overexpressed *ndr1* in the YSL (*ndr1* mRNA>YSL) of SP600125-treated embryos in order to analyze the relationship between these two signaling pathways. Interestingly, *sox32* expression in MMCs was not observed in *ndr1* mRNA>YSL embryos treated with SP600125 at 4.7 hpf (Fig. 7A-B′). In addition, mean DNB and DCN values in MMCs were not reduced in SP600125-treated embryos as compared with those in DMSO-treated control embryos, despite *ndr1* mRNA overexpression in the YSL (Fig. 7C,D).

We next investigated the hierarchical relationship between Smad and non-Smad JNK signaling pathways with respect to nuclear movement via a dominant-negative (dn) form of Smad2, which is mutated in the C-terminus sites normally subject to phosphorylation by receptor tyrosine kinases (Jia et al., 2008). A previous study reported that overexpression of *dn smad2* mRNA abolishes *sox32* induction by ectopic Nodal signaling in zebrafish embryos (Jia et al., 2008). Similarly, we found that *sox32* expression was significantly reduced in *dn smad2*-overexpressing embryos (Fig. 7E-G). In addition, nuclear movement in *dn smad2*-

Development (2017) 144, 4015-4025 doi:10.1242/dev.151746

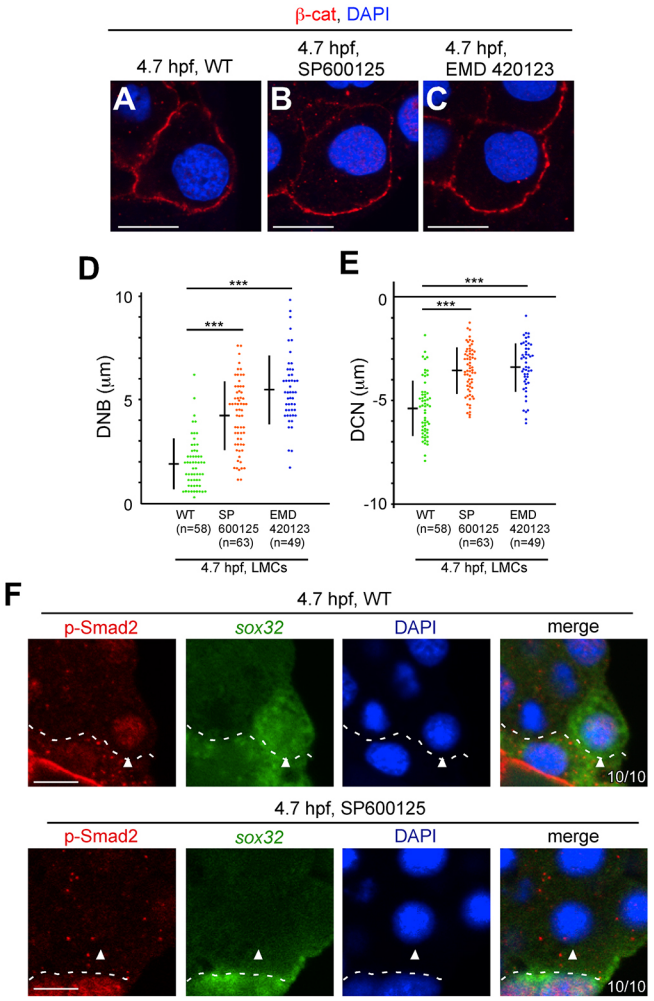

Fig. 5. Inhibition of JNK signaling suppresses nuclear movement and p-Smad2 nuclear translocation in LMCs. (A-C) Transverse sections of WT, SP600125-treated and EMD 420123-treated embryos; cell membrane and nuclei were visualized by β-cat and DAPI staining, respectively at 4.7 hpf. (D,E) DNB and DCN in LMCs were measured in WT and inhibitor-treated embryos. ***P<0.001. (F) Transverse sections of WT and SP600125-treated embryos; p-Smad2 and *sox32* were visualized by immunohistochemical staining and FISH, respectively. The number of embryos examined is shown bottom right. Arrowheads indicate nuclei in LMCs. Dashed lines indicate the boundary between the blastoderm and the YSL. Scale bars: 10 μm.

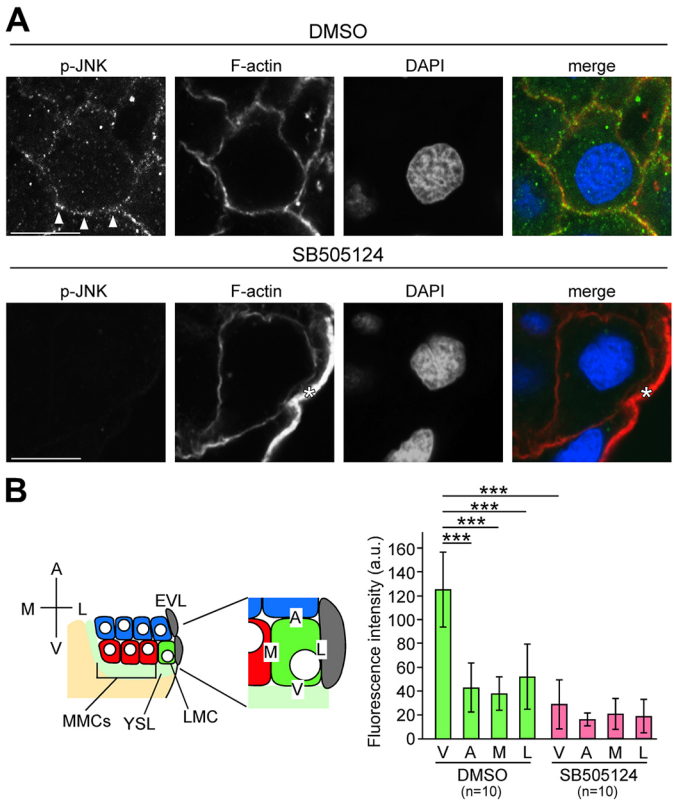

Fig. 6. JNK is activated by Nodal from the YSL. (A) Transverse sections of DMSO-treated control and SB505124-treated embryos; p-JNK and F-actin were visualized by immunohistochemical staining and phalloidin, respectively at 4.7 hpf. Fluorescent signals are displayed as grayscale images. Arrowheads indicate p-JNK fluorescence on the boundary between the YSL and LMCs. Asterisk indicates the cell membrane of EVL cells. Scale bars: 10 μm. (B) Fluorescence intensities were measured along the cell membrane on the boundaries between the YSL and LMCs (V), on cells located animal-pole side and LMCs (A), EVL and LMCs (L), or MMCs and LMCs (M). Error bars represent s.d. of ten measurements. *n*, number of nuclei examined. ***P<0.001.

overexpressing embryos was unchanged compared with that in *nlacZ*-overexpressing embryos (Fig. 7H-K), further confirming that nuclear movement regulated by non-Smad JNK signaling is independent of the Smad signaling pathway.

Nuclear movement toward the YSL is associated with nuclear translocation of Smad2

As nuclear movement toward the YSL is coincident with p-Smad2 nuclear translocation during zebrafish endoderm specification (Fig. 1J, Fig. 3F, Fig. 5F), we hypothesized that these events are directly linked, i.e. that the increase in the nuclear proportion of Smad2 is a consequence of nuclear movement toward the YSL. We visualized Smad2 nuclear translocation using time-lapse confocal live imaging in zebrafish embryos, as previously reported (Harvey and Smith, 2009; Dubrulle et al., 2015). We co-injected *EGFP-smad2*, *smad4a*, membrane-bound *RFP* (*mb-RFP*) and *H2B-mCherry* mRNAs at the one-cell stage, then injected *nlacZ* or *ndr1* mRNA with dextran-Alexa Fluor 594 into the YSL at 3 hpf; EGFP-Smad2 fluorescence was observed in MMCs at 5.3-6.0 hpf (Fig. S5). The nuclear/cytoplasmic ratio of EGFP-Smad2 fluorescence gradually increased as the nucleus moved toward the YSL when *ndr1*, but not *nlacZ*, mRNA was injected into the YSL (Fig. 8A-C). Our results suggest that nuclear movement toward the YSL is associated with Smad2 nuclear translocation.

DISCUSSION

A model of the Nodal signaling pathway leading to endoderm specification

It is well known that induction of both endoderm and mesoderm in early vertebrate development is regulated by Nodal-Smad2/3 signaling pathways (Schier, 2009). The endoderm and mesoderm may arise from single marginal cells in zebrafish embryos at the blastula stage, and it appears that the fate of marginal cells is determined by the strength of Nodal signaling (Fukuda and Kikuchi, 2005; Zorn and Wells, 2009). However, regulation of Nodal signaling strength in the marginal cells has not yet been fully elucidated. In this study, we arrived at four conclusions. First, Nodal signaling is essential for nuclear movement toward the YSL, whereas nuclear envelope proteins are involved in this movement through MT formation. Second, positioning of the MTOC is

Development (2017) 144, 4015-4025 doi:10.1242/dev.151746

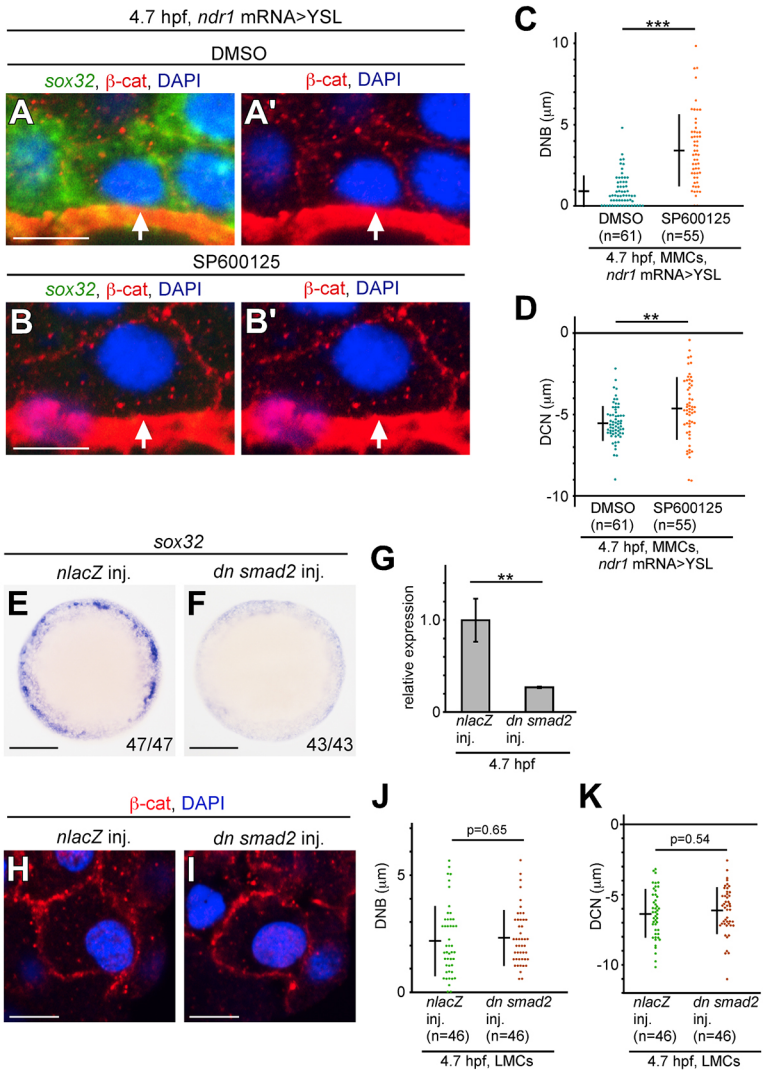

Fig. 7. Nuclear movement is regulated by non-Smad JNK signaling independent of Smad signaling. (A-B′) Transverse sections of *ndr1* mRNA>YSL embryos treated with DMSO as control (A,A′) and SP600125 (B,B′); the cell membrane, nucleus and *sox32* mRNA were visualized by β-cat staining, DAPI staining and FISH, respectively at 4.7 hpf. Arrows indicate nuclei in MMCs. (C,D) Mean DNB and DCN values in MMCs of *ndr1* mRNA>YSL embryos treated with SP600125 or DMSO at 4.7 hpf. *n*, number of nuclei examined. ***P<0.001, **P<0.05. (E,F) WISH of *sox32* expression in *nlacZ* or *dn smad2* mRNA-overexpressing embryos at 5.3 hpf. The number of embryos is shown bottom right. Animal pole views. (G) *sox32* expression in *nlacZ* or *dn smad2* mRNA-overexpressing embryos at 5.3 hpf measured by qPCR. Expression level of *nlacZ*-overexpressing embryos is set as 1.0. **P<0.05. Error bars represent s.d. of three independent experiments. (H,I) Transverse sections of *nlacZ*- and *dn smad2*-overexpressing embryos; the cell membrane and nuclei were visualized by β-cat and DAPI staining, respectively at 4.7 hpf. (J,K) DNB and DNC in LMCs were measured in *nlacZ*- and *dn smad2*-overexpressing embryos at 4.7 hpf. *n*, number of nuclei examined. Scale bars: 10 μm in A-B′,H,I; 200 μm in E,F.

regulated by Nodal signaling and nuclear envelope proteins. Third, the non-Smad JNK signaling pathway, which acts downstream of Nodal signaling, regulates nuclear movement independently of Smad2. Fourth, this nuclear movement is associated with Smad signal transduction toward the nucleus. Based on our results, we propose a model for how these signal transduction pathways result in endoderm specification of LMCs (Fig. 9). Nodal activates two signaling pathways: one mediated by Smad2 and the other mediated by JNK. Activation of JNK, which is a different pathway from that involving phosphorylation of Smad, induces nuclear movement toward the YSL, and MTOC reorientation is involved in this movement. This nuclear movement mediates the translocation of p-Smad2 into the nucleus, which then initiates the molecular programs for endoderm specification. Finally, activation of *sox32* drives cellular fate toward endoderm differentiation. In our model, Nodal signaling should be higher in LMCs than in other marginal cells between 4.0 and 4.7 hpf, since nuclear movement occurs in LMCs at 4.7 hpf. Consistent with this idea, we found that expression of *gata5* and *sox32*, which are thought to be activated by high Nodal signaling (Alexander et al., 1999; Rodaway et al., 1999; Ober et al., 2003), was restricted to the LMCs at 4.7 hpf (Fig. 1H).

It is well characterized that mitogen-activated protein kinases (MAPKs), a family of serine/threonine protein kinases, are part of the downstream signaling of TGFβ, and consist of three subgroups: Erk, p38 and JNK. Previous studies have revealed that MAPKs phosphorylate the linker region of Smad2/3 by activation of TGFβ, which, in turn, blocks the nuclear translocation of Smad2/3 (Massague, 2003; Mori et al., 2004; Wrighton et al., 2009). In *Xenopus* embryos, overexpression of Smad2 with a mutation in the linker region of phosphorylation sites leads to nuclear accumulation of the mutated Smad2. This prolongs the response time of endogenous mesodermal genes to activin signaling (Grimm and Gurdon, 2002). In zebrafish embryos, overexpression of Smad2 phosphorylation mutants results in an increase in mesoderm and endoderm genes (Liu et al., 2013), suggesting that Smad2 phosphorylation by MAPKs has an inhibitory function. On the other hand, we showed that inhibition of JNK by SP600125 resulted in a reduction in *sox32* expression (Fig. S3). Therefore, JNK does not seem to be involved in endoderm gene induction via direct phosphorylation of the linker region of Smad2. Similar to the endoderm marker *sox32*, the expression level of a mesoderm marker gene, *ta*, was significantly reduced in JNK-inhibited and *C-syne2a*-overexpressing embryos (Figs S2 and S3). However, since *ta* expression was downregulated only on the dorsal side of Nodal signaling-deficient embryos (Feldman et al., 1998; Gritsman et al., 1999), it is possible that JNK and nuclear envelope proteins regulate *ta* expression via Nodal-independent signaling pathway.

Development (2017) 144, 4015-4025 doi:10.1242/dev.151746

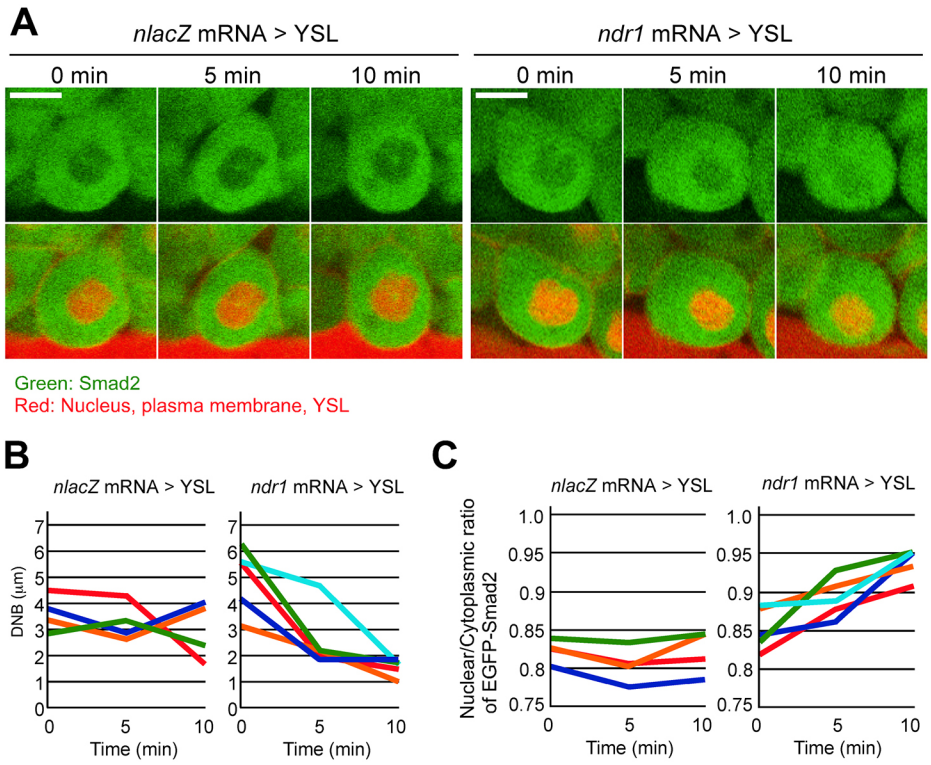

Fig. 8. Visualization of Smad2 during nuclear movement. (A) Time-lapse confocal live imaging of EGFP-Smad2 in MMCs of *nlacZ* mRNA>YSL or *ndr1* mRNA>YSL embryos. Scale bars: 10 μm. (B,C) DNB values (B) and nuclear/cytoplasmic ratio of EGFP-Smad2 fluorescence (C) of four or five independent nuclei (colored lines) in MMCs of *nlacZ* mRNA>YSL or *ndr1* mRNA>YSL embryos.

Thus far, only one study has reported on the relationship between nuclear positioning and asymmetric signaling, which was in the zebrafish retinal neuroepithelium (Del Bene et al., 2008). This report showed that during interkinetic nuclear migration, the strength of Notch signaling is dependent on nuclear movement along the apical-basal axis of the neuroepithelium in radial glia cells (Del Bene et al., 2008). Accordingly, expression of *notch1a* and *deltaB/C* was found to be higher at the apical and basal surfaces of the retina, respectively (Del Bene et al., 2008). However, we showed that both Smad and non-Smad signaling pathways, cooperatively but independently, determine the specification of endoderm fate in zebrafish blastulae. Our model presents a new system of signaling transduction downstream of TGFβ, which is associated with nuclear movement.

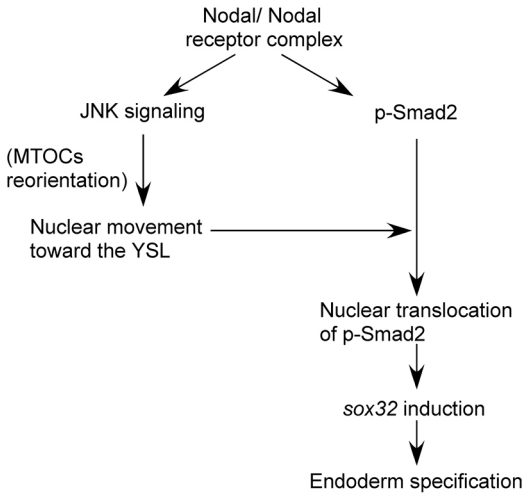

Fig. 9. Model of Nodal signaling pathways leading to endoderm specification in zebrafish LMCs. Nodal activates two signaling pathways – mediated by Smad2 and JNK. Activation of JNK induces nuclear movement toward the YSL, which involves MTOC reorientation. This movement mediates the translocation of p-Smad2, in the second pathway, into the nucleus, which initiates molecular programs for endoderm specification, culminating in the activation of *sox32* that drives endoderm differentiation.

Nuclear movement by cytoskeletal components

Nuclear movement is mainly controlled by cytoskeletal elements (MTs and actin microfilaments) and associated motor proteins (Bone and Starr, 2016; Gundersen and Worman, 2013; Dupin and Etienne-Manneville, 2011). It has been reported that actin microfilaments and acto-myosin contraction are involved in nuclear movement; for example, in cultured migrating fibroblasts and in the radial migration of neural precursors, mainly through pushing forces (Gundersen and Worman, 2013; Dupin and Etienne-Manneville, 2011). Based on these previous reports, we examined F-actin formation in WT and Nodal signaling-deficient embryos by phalloidin staining at 4.7 hpf. However, no obvious differences in F-actin formation were observed (Fig. 6). In addition, inhibition of RhoA, Rac1 and Cdc42, which function as regulators of actin dynamics downstream of TGFβ signaling (Moustakas and Heldin, 2005; Derynck and Zhang, 2003; Mu et al., 2012), had no effect on endoderm specification (data not shown). These results suggest that nuclear movement in zebrafish LMCs during endoderm specification is an actin-independent process.

Our results indicated that overexpression of the dominant-negative form of Syne2a inhibits nuclear movement. In addition, Syne2a regulates the attachment of MTOCs to the nucleus and it necessary for MT formation in LMCs, suggesting that LINC complex proteins are involved in nuclear positioning via regulation of MT formation. In zebrafish photoreceptors, nuclear movement is regulated by the motor protein dynein complex via MTs, and results in differential activation of Notch signaling along an apical-basal signaling gradient (Del Bene et al., 2008). However, it has recently been proposed that the Nodal signaling pathway is mediated through endocytosis. Zebrafish Rab5ab, a member of the RAB family of small GTPases, has been identified as an essential factor for Nodal

Development (2017) 144, 4015-4025 doi:10.1242/dev.151746

signaling (Kenyon et al., 2015). Furthermore, MTs and associated motor proteins are necessary for the transportation of cellular components, including endocytic vesicles and organelles. Consequently, we did not analyze the function of motor proteins in the nuclear movement of LMCs as it is difficult to exclude the possibility that inhibition of motor proteins, such as dynein and kinesin, affects endocytic vesicle-mediated Nodal signaling.

MTOC reorientation and nuclear movement are regulated by the JNK signaling pathway

The significance of MTOC positioning in nuclear movement has been investigated in several studies: male and female pronuclei migration in newly fertilized *C. elegans* eggs, oocyte migration in the *Drosophila* egg chamber, and interkinetic nuclear migration in the vertebrate neuroepithelium (Gundersen and Worman, 2013; Starr, 2009). These studies revealed that the connection between the nucleus and MTs is mediated by LINC complex proteins, and that MTOC positioning appears to be a crucial factor in MT-mediated nuclear movement. In our study, we showed that one of the MTOCs in LMCs shifted closer to the YSL during endoderm specification (Fig. 4). In addition, both MTOC reorientation and nuclear movement were blocked when JNK signaling was inhibited (Figs 4 and 5). Our data, in combination with previous results, suggest that nuclear movement toward the YSL is elicited by the reorientation of the MTOC toward the YSL.

Immunological synapse formation between a T cell and an antigen-presenting cell is associated with MTOC reorientation, and novel and atypical members of protein kinase C family are involved in MTOC reorientation of T cells (Huse, 2012). In natural killer cells, on the other hand, JNK activation is required for cytotoxicity through MTOC reorientation (Li et al., 2008), suggesting that MAPKs are associated with MTOC reorientation. We have already shown that the Fgf/Mek/Erk signaling pathway negatively and positively regulates endoderm and mesoderm formation, respectively (Mizoguchi et al., 2006), suggesting that the Mek/Erk signaling pathway is not involved in the reorientation of MTOCs. In this study, we found that inhibition of p38 has no effect on endoderm specification (data not shown), and that Nodal-induced JNK activation regulates MTOC reorientation. However, further studies are required to elucidate the mechanism by which Nodal/JNK signaling regulates MTOC reorientation, which in turn contributes to nuclear movement.

MATERIALS AND METHODS

Zebrafish husbandry and drug treatments

All zebrafish experiments were approved by the Hiroshima University Animal Research Committee (Permit Number: F16-1). Wild-type (WT) AB strain zebrafish embryos were incubated in 1/3 Ringer's solution at 28.5°C (Mizoguchi et al., 2006) and staged according to Kimmel et al. (1995).

Drug treatments

WT zebrafish embryos were dechorionated with 0.2 mg/ml pronase (Sigma-Aldrich) in 1/3 Ringer's solution at the one-cell stage (Mizoguchi et al., 2006). The embryos were then treated with inhibitors at 28.5°C or with an equivalent amount of DMSO during the 1- to 4-cell stage until fixation. The following inhibitors were used (all dissolved in DMSO): SB505124 (50 µM, Sigma-Aldrich), SB431542 (100 µM, Tocris Bioscience), SP600125 (10 µM, Cayman Chemical), EMD 420123 (50 µM, Merck Millipore), SB203580 (20 µM and 60 µM, Merck Millipore), NF-κB activation inhibitor (50 nM, Merck Millipore), ML141 (10 µM and 25 µM, Sigma-Aldrich), Y27632 (50 µM, Focus Biomolecules), LY294002 (10 µM, Merck Millipore) and NSC23766 (150 µM and 300 µM, Merck Millipore). WT embryos with chorion were treated with nocodazole (66 µM, Sigma-Aldrich) (Brunet et al., 2013) from 3.8 hpf, and were fixed at 4.7 hpf.

mRNA injections

pCS2+ vector carrying *ndr1* cDNA (Rebagliati et al., 1998), *C-syne2a* (Tsujikawa et al., 2007), *dn smad2* (Jia et al., 2008), *EGFP-smad2* (Dubrulle et al., 2015), *smad4a* (Hsu et al., 2011), *mb-RFP* (Iioka et al., 2004), *mb-Venus* (Kinoshita et al., 2003), *H2B-mCherry* (Shiomi et al., 2017) or nuclear *lacZ* (*nlacZ*) was used. Capped mRNA was synthesized using SP6 mMESSAGE mMACHINE (Ambion). Embryos were injected with the following mRNAs: *C-syne2a* (500 pg), *dn smad2* (600 pg), *H2B-mCherry* (80 pg or 100 pg), *mb-Venus* (100 pg), *mb-RFP* (80 pg), *EGFP-smad2* (100 pg), *smad4a* (100 pg) or *nlacZ* (500 pg or 600 pg) at the one-cell stage. For overexpression experiments in the YSL, *ndr1* or *nlacZ* mRNA (2880 pg each) with dextran-Alexa Fluor 594 (Thermo Fisher Scientific) was injected into the YSL at 3 hpf.

WISH, immunohistochemistry and FISH

WISH was performed as previously described (Westerfield, 1993), and riboprobes were prepared according to published methods (Westerfield, 1993).

Immunohistochemistry was performed as previously described (Hirose et al., 2013) with two overnight fixations, with the exception of anti-α-tubulin antibody staining, where embryos were fixed with 3.7% formaldehyde and 0.25% glutaraldehyde in a microtubule assembly buffer (80 mM K-PIPES pH 6.8, 5 mM EGTA, 1 mM $MgCl_2$, 0.2% Triton X-100) (Topczewski and Solnica-Krezel, 1999). For double staining with anti-p-JNK and Rhodamine-phalloidin, embryos were fixed with 3.7% formaldehyde in PBS containing 0.1% Tween 20 (PBSTw) for 2 h at room temperature; dehydration was omitted. Rhodamine-phalloidin (R415, Thermo Fisher Scientific) was used at 1:100 for actin filament staining.

When FISH and immunohistochemistry were both required, immunohistochemistry was performed after FISH. Following hybridization with the *sox32* RNA probe, the embryos were sectioned and incubated in anti-digoxigenin-POD Fab fragments (Roche), diluted at 1:500 with 8% sheep serum in PBSTw. After the tyramide signal amplification reaction, which was performed as previously described (Lauter et al., 2011), the sections were treated with blocking buffer, then incubated with primary antibody diluted in the same buffer. The following primary antibodies were used: anti-β-catenin rabbit polyclonal antibody at 1:300 (C-2206, Sigma-Aldrich); anti-γ-tubulin mouse monoclonal antibody at 1:500 (T6557, Sigma-Aldrich); anti-α-tubulin mouse monoclonal antibody at 1:5000 (T5168, Sigma-Aldrich); anti-phospho-Smad2 (Ser465/467) rabbit monoclonal antibody at 1:250 (04-953, Merck Millipore); and anti-phospho-SAPK/JNK rabbit polyclonal antibody at 1:100 (#9251, Cell Signaling Technology). The following secondary antibodies were used (all at 1:500): Alexa Fluor 488 goat anti-rabbit IgG antibody (A11034, Thermo Fisher Scientific); Alexa Fluor 594 goat anti-rabbit IgG antibody (A11037, Thermo Fisher Scientific); and Alexa Fluor 488 goat anti-mouse IgG antibody (A11029, Thermo Fisher Scientific). Nuclei were stained with 4′,6-diamidino-2-phenylindole (DAPI) at 1:1000.

Quantitative real-time PCR (qPCR) analyses

qPCR analyses were performed as previously described (Hirose et al., 2013). Total RNA was extracted from 20-40 embryos at 4.7 or 5.3 hpf using TRIzol (Thermo Fisher Scientific), and 500 ng DNase-treated RNA was reverse transcribed using olgo(dT) primers and reverse transcriptase XL (Takara). qPCR for four genes (*ndr1*, *ndr2*, *ta* and *sox32*) was performed in triplicate or tetraplicate with the Thermal Cycler Dice Real-Time System II and SYBR Premix Ex Taq II (Takara), according to the manufacturer's instructions. Zebrafish *ribosomal protein L13a* (*rpl13a*) was used as a reference gene. qPCR primers are listed in Table S1.

Imaging and image analysis

Images were acquired using an Olympus FV1000-D confocal microscope system. Confocal live imaging was performed as previously described (Mizoguchi et al., 2008). Confocal time-lapse imaging was performed on the same confocal microscope using a 60× water-immersion lens. We recorded *z*-stacks (0.62 µm steps) at 5 min intervals, and analyzed the images using ImageJ software (NIH). The p-JNK intensities at the cell membranes of LMCs were analyzed using ImageJ by measuring the mean gray value of a three-pixel-wide line drawn along the cell membrane on the boundary between the

Development (2017) 144, 4015-4025 doi:10.1242/dev.151746

YSL and LMCs, between cells located at the animal pole side and LMCs, between the EVL and LMCs, or between MMCs and LMCs (Morrissey et al., 2016). Cytoplasmic background signals were subtracted from each of the mean gray values. Average values and standard deviations were determined from ten LMCs of DMSO-treated or SB505124-treated embryos. To measure cytoplasmic area occupied by MTs, one fluorescent image of MTs was converted to grayscale, and the area of MTs and of cytoplasm were determined by threshold analysis and freehand selection in ImageJ, respectively (Wadsworth and McGrail, 1990; Craig et al., 2010).

Statistical analyses

Data are expressed as averages from repeated experiments with standard deviation. Statistical significance was determined by Student's *t*-test. $P<0.05$ was considered statistically significant.

Acknowledgements

We thank Dr Anming Meng for pCS2-*dn smad2*; Dr Noriyuki Kinoshita for pCS2-*mb-RFP* and pCS2-*mb-Venus*; Dr Hiroshi Kimura for pCS2-*H2B-mCherry*; the Institute for Amphibian Biology at Hiroshima University for cryostat sectioning and qPCR; and the members of the Y.K. and Atsushi Suzuki laboratories at Hiroshima University for helpful discussion and critical comments.

Competing interests

The authors declare no competing or financial interests.

Author contributions

Conceptualization: S.H., Y.K.; Methodology: S.H.; Formal analysis: S.H.; Investigation: S.H., S.A.; Writing - original draft: S.H., Y.K.; Writing - review & editing: S.H., S.A., Y.K.; Visualization: S.H.; Supervision: Y.K.; Project administration: Y.K.; Funding acquisition: S.H.

Funding

This work was supported by a Hiroshima University Grant-in-Aid for Exploratory Research (Researcher Support of Young Scientists) to S.H.

Supplementary information

Supplementary information available online at
http://dev.biologists.org/lookup/doi/10.1242/dev.151746.supplemental

References

Alexander, J., Rothenberg, M., Henry, G. L. and Stainier, D. Y. R. (1999). casanova plays an early and essential role in endoderm formation in zebrafish. *Dev. Biol.* **215**, 343-357.

Bennett, B. L., Sasaki, D. T., Murray, B. W., O'leary, E. C., Sakata, S. T., Xu, W., Leisten, J. C., Motiwala, A., Pierce, S., Satoh, Y. et al. (2001). SP600125, an anthrapyrazolone inhibitor of Jun N-terminal kinase. *Proc. Natl. Acad. Sci. USA* **98**, 13681-13686.

Bone, C. R. and Starr, D. A. (2016). Nuclear migration events throughout development. *J. Cell Sci.* **129**, 1951-1961.

Brunet, T., Bouclet, A., Ahmadi, P., Mitrossilis, D., Driquez, B., Brunet, A.-C., Henry, L., Serman, F., Béalle, G., Ménager, C. et al. (2013). Evolutionary conservation of early mesoderm specification by mechanotransduction in Bilateria. *Nat. Commun.* **4**, 2821.

Callahan, J. F., Burgess, J. L., Fornwald, J. A., Gaster, L. M., Harling, J. D., Harrington, F. P., Heer, J., Kwon, C., Lehr, R., Mathur, A. et al. (2002). Identification of novel inhibitors of the transforming growth factor beta1 (TGF-beta1) type 1 receptor (ALK5). *J. Med. Chem.* **45**, 999-1001.

Craig, S. E., Thummel, R., Ahmed, H., Vasta, G. R., Hyde, D. R. and Hitchcock, P. F. (2010). The zebrafish galectin Drgal1-l2 is expressed by proliferating Müller glia and photoreceptor progenitors and regulates the regeneration of rod photoreceptors. *Invest. Ophthalmol. Vis. Sci.* **51**, 3244-3252.

Cuenda, A., Rouse, J., Doza, Y. N., Meier, R., Cohen, P., Gallagher, T. F., Young, P. R. and Lee, J. C. (1995). SB 203580 is a specific inhibitor of a MAP kinase homologue which is stimulated by cellular stresses and interleukin-1. *FEBS Lett.* **364**, 229-233.

Dacosta Byfield, S., Major, C., Laping, N. J. and Roberts, A. B. (2004). SB-505124 is a selective inhibitor of transforming growth factor-beta type I receptors ALK4, ALK5, and ALK7. *Mol. Pharmacol.* **65**, 744-752.

Del Bene, F., Wehman, A. M., Link, B. A. and Baier, H. (2008). Regulation of neurogenesis by interkinetic nuclear migration through an apical-basal notch gradient. *Cell* **134**, 1055-1065.

Derynck, R. and Zhang, Y. E. (2003). Smad-dependent and Smad-independent pathways in TGF-beta family signalling. *Nature* **425**, 577-584.

Dickmeis, T., Mourrain, P., Saint-Etienne, L., Fischer, N., Aanstad, P., Clark, M., Str Hle, U. and Rosa, F. (2001). A crucial component of the endoderm formation pathway, CASANOVA, is encoded by a novel sox-related gene. *Genes Dev.* **15**, 1487-1492.

Di Guglielmo, G. M., Le Roy, C., Goodfellow, A. F. and Wrana, J. L. (2003). Distinct endocytic pathways regulate TGF-beta receptor signalling and turnover. *Nat. Cell Biol.* **5**, 410-421.

Dubrulle, J., Jordan, B. M., Akhmetova, L., Farrell, J. A., Kim, S. H., Solnica-Krezel, L. and Schier, A. F. (2015). Response to Nodal morphogen gradient is determined by the kinetics of target gene induction. *Elife* **4**, e05042.

Dupin, I. and Etienne-Manneville, S. (2011). Nuclear positioning: mechanisms and functions. *Int. J. Biochem. Cell Biol.* **43**, 1698-1707.

Feldman, B., Gates, M. A., Egan, E. S., Dougan, S. T., Rennebeck, G., Sirotkin, H. I., Schier, A. F. and Talbot, W. S. (1998). Zebrafish organizer development and germ-layer formation require nodal-related signals. *Nature* **395**, 181-185.

Fukuda, K. and Kikuchi, Y. (2005). Endoderm development in vertebrates: fate mapping, induction and regional specification. *Dev. Growth Differ.* **47**, 343-355.

Gao, Y., Dickerson, J. B., Guo, F., Zheng, J. and Zheng, Y. (2004). Rational design and characterization of a Rac GTPase-specific small molecule inhibitor. *Proc. Natl. Acad. Sci. USA* **101**, 7618-7623.

Grimm, O. H. and Gurdon, J. B. (2002). Nuclear exclusion of Smad2 is a mechanism leading to loss of competence. *Nat. Cell Biol.* **4**, 519-522.

Gritsman, K., Zhang, J., Cheng, S., Heckscher, E., Talbot, W. S. and Schier, A. F. (1999). The EGF-CFC protein one-eyed pinhead is essential for nodal signaling. *Cell* **97**, 121-132.

Gundersen, G. G. and Worman, H. J. (2013). Nuclear positioning. *Cell* **152**, 1376-1389.

Han, Z., Boyle, D. L., Chang, L., Bennett, B., Karin, M., Yang, L., Manning, A. M. and Firestein, G. S. (2001). c-Jun N-terminal kinase is required for metalloproteinase expression and joint destruction in inflammatory arthritis. *J. Clin. Invest.* **108**, 73-81.

Harvey, S. A. and Smith, J. C. (2009). Visualisation and quantification of morphogen gradient formation in the zebrafish. *PLoS Biol.* **7**, e1000101.

Hayes, S., Chawla, A. and Corvera, S. (2002). TGF beta receptor internalization into EEA1-enriched early endosomes: role in signaling to Smad2. *J. Cell Biol.* **158**, 1239-1249.

Hirose, K., Shimoda, N. and Kikuchi, Y. (2013). Transient reduction of 5-methylcytosine and 5-hydroxymethylcytosine is associated with active DNA demethylation during regeneration of zebrafish fin. *Epigenetics* **8**, 899-906.

Hsu, R.-J., Lin, C.-C., Su, Y.-F. and Tsai, H.- J. (2011). dickkopf-3-related gene regulates the expression of zebrafish myf5 gene through phosphorylated p38a-dependent Smad4 activity. *J. Biol. Chem.* **286**, 6855-6864.

Huse, M. (2012). Microtubule-organizing center polarity and the immunological synapse: protein kinase C and beyond. *Front. Immunol.* **3**, 235.

Iioka, H., Ueno, N. and Kinoshita, N. (2004). Essential role of MARCKS in cortical actin dynamics during gastrulation movements. *J. Cell Biol.* **164**, 169-174.

Inman, G. J., Nicolás, F. J., Callahan, J. F., Harling, J. D., Gaster, L. M., Reith, A. D., Laping, N. J. and Hill, C. S. (2002). SB-431542 is a potent and specific inhibitor of transforming growth factor-beta superfamily type I activin receptor-like kinase (ALK) receptors ALK4, ALK5, and ALK7. *Mol. Pharmacol.* **62**, 65-74.

Jia, S., Ren, Z., Li, X., Zheng, Y. and Meng, A. (2008). smad2 and smad3 are required for mesendoderm induction by transforming growth factor-beta/nodal signals in zebrafish. *J. Biol. Chem.* **283**, 2418-2426.

Kenyon, E. J., Campos, I., Bull, J. C., Williams, P. H., Stemple, D. L. and Clark, M. D. (2015). Zebrafish Rab5 proteins and a role for Rab5ab in nodal signalling. *Dev. Biol.* **397**, 212-224.

Kikuchi, Y., Agathon, A., Alexander, J., Thisse, C., Waldron, S., Yelon, D., Thisse, B. and Stainier, D. Y. (2001). casanova encodes a novel Sox-related protein necessary and sufficient for early endoderm formation in zebrafish. *Genes Dev.* **15**, 1493-1505.

Kimmel, C. B., Ballard, W. W., Kimmel, S. R., Ullmann, B. and Schilling, T. F. (1995). Stages of embryonic development of the zebrafish. *Dev. Dyn.* **203**, 253-310.

Kinoshita, N., Iioka, H., Miyakoshi, A. and Ueno, N. (2003). PKC delta is essential for Dishevelled function in a noncanonical Wnt pathway that regulates Xenopus convergent extension movements. *Genes Dev.* **17**, 1663-1676.

Laping, N. J., Grygielko, E., Mathur, A., Butter, S., Bomberger, J., Tweed, C., Martin, W., Fornwald, J., Lehr, R., Harling, J. et al. (2002). Inhibition of transforming growth factor (TGF)-beta1-induced extracellular matrix with a novel inhibitor of the TGF-beta type I receptor kinase activity: SB-431542. *Mol. Pharmacol.* **62**, 58-64.

Lauter, G., Söll, I. and Hauptmann, G. (2011). Multicolor fluorescent in situ hybridization to define abutting and overlapping gene expression in the embryonic zebrafish brain. *Neural Dev.* **6**, 10.

Li, C., Ge, B., Nicotra, M., Stern, J. N. H., Kopcow, H. D., Chen, X. and Strominger, J. L. (2008). JNK MAP kinase activation is required for MTOC and granule polarization in NKG2D-mediated NK cell cytotoxicity. *Proc. Natl. Acad. Sci. USA* **105**, 3017-3022.

Liu, X., Xiong, C., Jia, S., Zhang, Y., Chen, Y.-G., Wang, Q. and Meng, A. (2013). Araf kinase antagonizes Nodal-Smad2 activity in mesendoderm development by directly phosphorylating the Smad2 linker region. *Nat. Commun.* **4**, 1728.
Massague, J. (2003). Integration of Smad and MAPK pathways: a link and a linker revisited. *Genes Dev.* **17**, 2993-2997.
Mizoguchi, T., Izawa, T., Kuroiwa, A. and Kikuchi, Y. (2006). Fgf signaling negatively regulates Nodal-dependent endoderm induction in zebrafish. *Dev. Biol.* **300**, 612-622.
Mizoguchi, T., Verkade, H., Heath, J. K., Kuroiwa, A. and Kikuchi, Y. (2008). Sdf1/Cxcr4 signaling controls the dorsal migration of endodermal cells during zebrafish gastrulation. *Development* **135**, 2521-2529.
Mori, S., Matsuzaki, K., Yoshida, K., Furukawa, F., Tahashi, Y., Yamagata, H., Sekimoto, G., Seki, T., Matsui, H., Nishizawa, M. et al. (2004). TGF-beta and HGF transmit the signals through JNK-dependent Smad2/3 phosphorylation at the linker regions. *Oncogene* **23**, 7416-7429.
Morrissey, M. A., Jayadev, R., Miley, G. R., Blebea, C. A., Chi, Q., Ihara, S. and Sherwood, D. R. (2016). SPARC promotes cell invasion in vivo by decreasing type IV collagen levels in the basement membrane. *PLoS Genet.* **12**, e1005905.
Moustakas, A. and Heldin, C. H. (2005). Non-Smad TGF-beta signals. *J. Cell Sci.* **118**, 3573-3584.
Mu, Y., Gudey, S. K. and Landström, M. (2012). Non-Smad signaling pathways. *Cell Tissue Res.* **347**, 11-20.
Nomura, M. and Li, E. (1998). Smad2 role in mesoderm formation, left-right patterning and craniofacial development. *Nature* **393**, 786-790.
Ober, E. A., Field, H. A. and Stainier, D. Y. R. (2003). From endoderm formation to liver and pancreas development in zebrafish. *Mech. Dev.* **120**, 5-18.
Penheiter, S. G., Mitchell, H., Garamszegi, N., Edens, M., Dor, J. J. E. and Leof, E. B. (2002). Internalization-dependent and -independent requirements for transforming growth factor beta receptor signaling via the Smad pathway. *Mol. Cell. Biol.* **22**, 4750-4759.
Rebagliati, M. R., Toyama, R., Fricke, C., Haffter, P. and Dawid, I. B. (1998). Zebrafish nodal-related genes are implicated in axial patterning and establishing left-right asymmetry. *Dev. Biol.* **199**, 261-272.
Rodaway, A., Takeda, H., Koshida, S., Broadbent, J., Price, B., Smith, J. C., Patient, R. and Holder, N. (1999). Induction of the mesendoderm in the zebrafish germ ring by yolk cell-derived TGF-beta family signals and discrimination of mesoderm and endoderm by FGF. *Development* **126**, 3067-3078.
Schier, A. F. (2009). Nodal morphogens. *Cold Spring Harb. Perspect. Biol.* **1**, a003459.
Shiomi, T., Muto, A., Hozumi, S., Kimura, H. and Kikuchi, Y. (2017). Histone H3 lysine 27 trimethylation leads to loss of mesendodermal competence during gastrulation in zebrafish ectodermal cells. *Zoolog. Sci.* **34**, 64-71.
Starr, D. A. (2009). A nuclear-envelope bridge positions nuclei and moves chromosomes. *J. Cell Sci.* **122**, 577-586.
Tobe, M., Isobe, Y., Tomizawa, H., Nagasaki, T., Takahashi, H. and Hayashi, H. (2003). A novel structural class of potent inhibitors of NF-kappa B activation: structure-activity relationships and biological effects of 6-aminoquinazoline derivatives. *Bioorg. Med. Chem.* **11**, 3869-3878.
Topczewski, J. and Solnica-Krezel, L. (1999). Cytoskeletal dynamics of the zebrafish embryo. *Methods Cell Biol.* **59**, 205-226.
Tsujikawa, M., Omori, Y., Biyanwila, J. and Malicki, J. (2007). Mechanism of positioning the cell nucleus in vertebrate photoreceptors. *Proc. Natl. Acad. Sci. USA* **104**, 14819-14824.
Vlahos, C. J., Matter, W. F., Hui, K. Y. and Brown, R. F. (1994). A specific inhibitor of phosphatidylinositol 3-kinase, 2-(4-morpholinyl)-8-phenyl-4H-1-benzopyran-4-one (LY294002). *J. Biol. Chem.* **269**, 5241-5248.
Wadsworth, P. and Mcgrail, M. (1990). Interphase microtubule dynamics are cell type-specific. *J. Cell Sci.* **95**, 23-32.
Weinstein, M., Yang, X., Li, C., Xu, X., Gotay, J. and Deng, C.-X. (1998). Failure of egg cylinder elongation and mesoderm induction in mouse embryos lacking the tumor suppressor smad2. *Proc. Natl. Acad. Sci. USA* **95**, 9378-9383.
Westerfield, M. (1993). *The Zebrafish Book: a Guide for the Laboratory Use of Zebrafish (Brachydanio rerio)*. Eugene, OR: University of Oregon Press.
Wrighton, K. H., Lin, X. and Feng, X.-H. (2009). Phospho-control of TGF-beta superfamily signaling. *Cell Res.* **19**, 8-20.
Zorn, A. M. and Wells, J. M. (2009). Vertebrate endoderm development and organ formation. *Annu. Rev. Cell Dev. Biol.* **25**, 221-251.

Figure S1

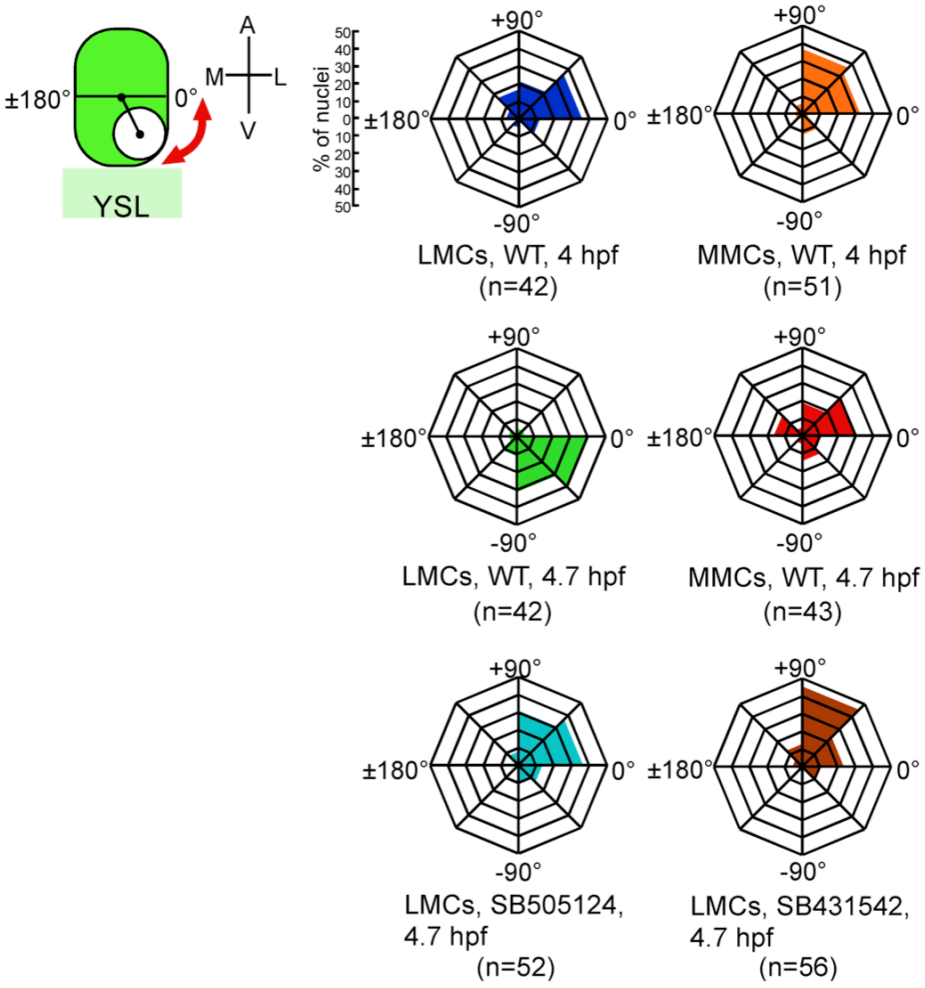

Figure S1. Nuclear positional changes in LMCs and MMCs between 4.0 and 4.7 hpf

Angles between the center of the cell and the nucleus relative to the medial-lateral axis were measured (red line). n = number of nuclei examined.

Figure S2

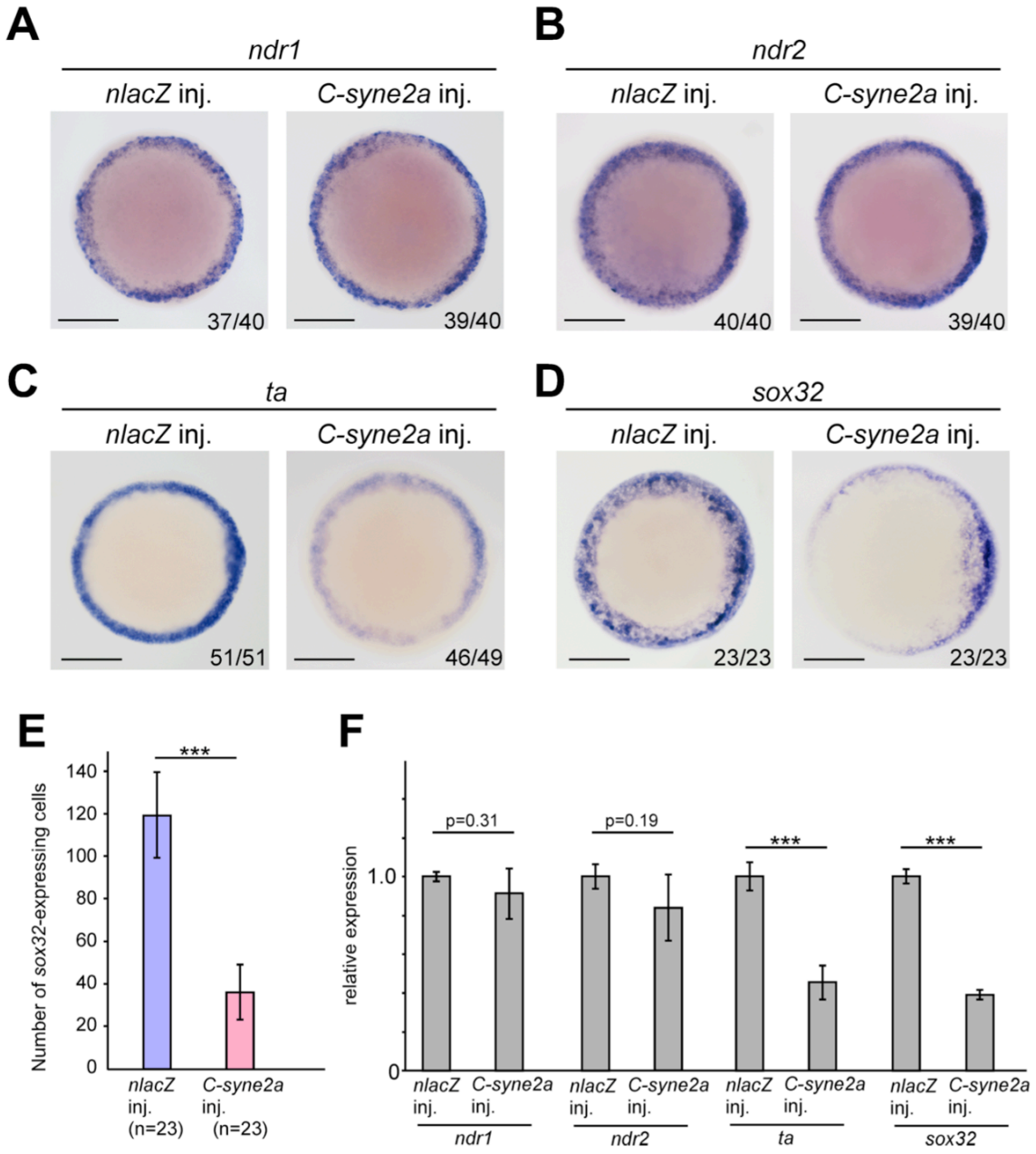

Figure S2. Expression of *ndr*, mesoderm, and endoderm genes in *C-syne2a*-overexpressing embryos

(A-D) Expression of *ndr1*, *ndr2*, *ta*, and *sox32* was examined by WISH in *nlacZ* or *C-syne2a* mRNA overexpressing embryos at 5.3 hpf. The number of embryos examined is shown at the lower right corner of each panel. Animal pole views. Scale

bars: 200 μm. (E) Number of *sox32*-expressing endodermal cells in *nlacZ*- or *C-syne2a*-overexpressing embryos at 5.3 hpf. n = number of embryos examined. ***$p < 0.001$. (F) Expression of *ndr1*, *ndr2*, *ta*, and *sox32* was examined by qPCR in *nlacZ* or *C-syne2a* mRNA-overexpressing embryos at 5.3 hpf. Error bars represent standard deviations of three or four independent experiments. ***$p < 0.001$.

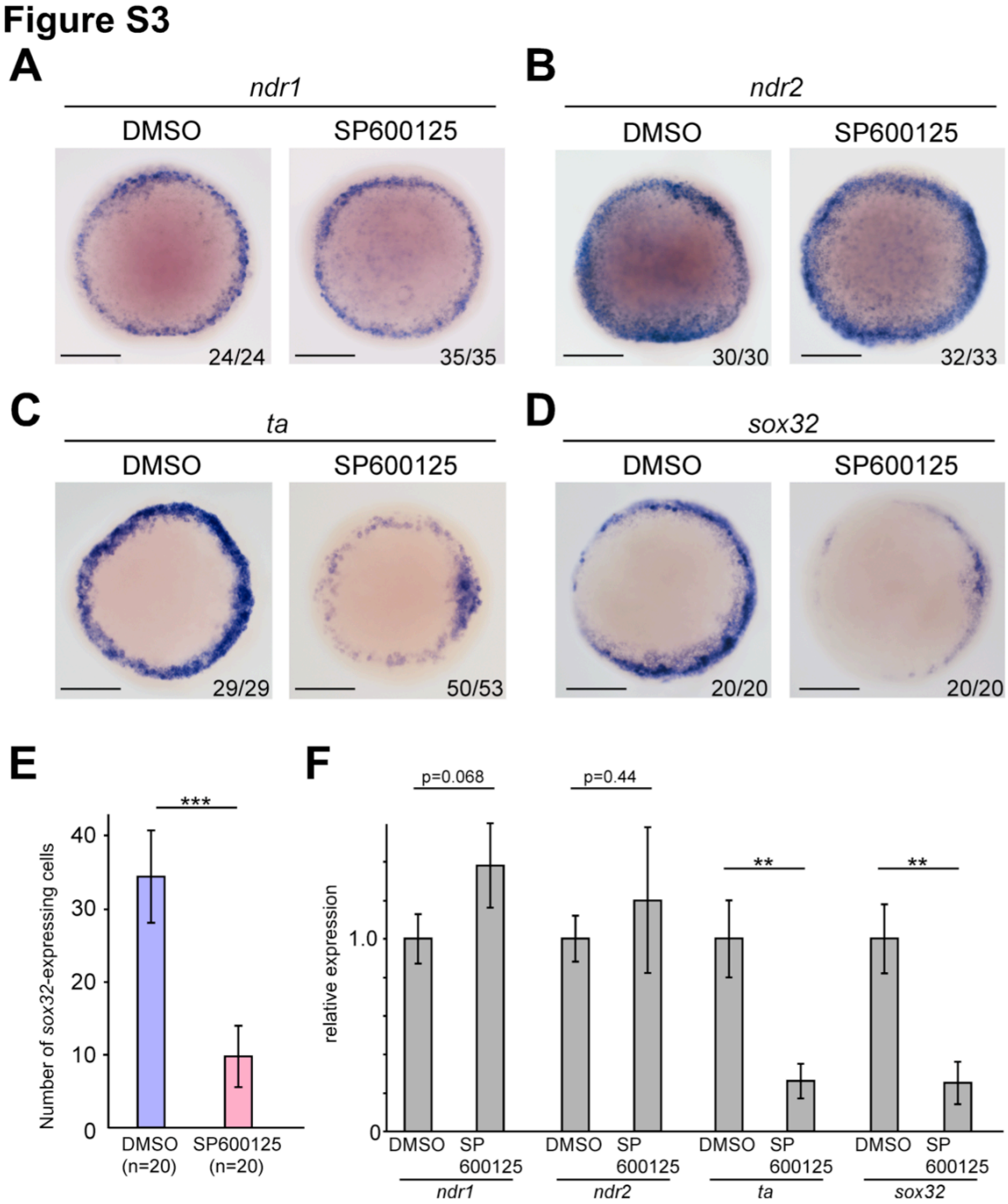

Figure S3. Expression of *ndr*, mesoderm, and endoderm genes in SP600125-treated embryos

(A-D) Expression of *ndr1*, *ndr2*, *ta*, and *sox32* was examined by whole-mount *in situ* hybridization in DMSO- or SP600125-treated embryos at 4.7 hpf. Number of embryos

examined is shown at the lower right corner of each panel. Animal pole views. Scale bars: 200 μm. (E) Number of *sox32*-expressing endodermal cell was counted in DMSO-, or SP600125-treated embryos. n = number of embryos examined. ***$p <$ 0.001. (F) Expression of *ndr1*, *ndr2*, *ta*, and *sox32* was examined by qPCR in DMSO- or SP600125-treated embryos at 4.7 hpf. Error bars represent standard deviations of three or four independent experiments. ***$p < 0.001$. ** $p < 0.05$.

Figure S4

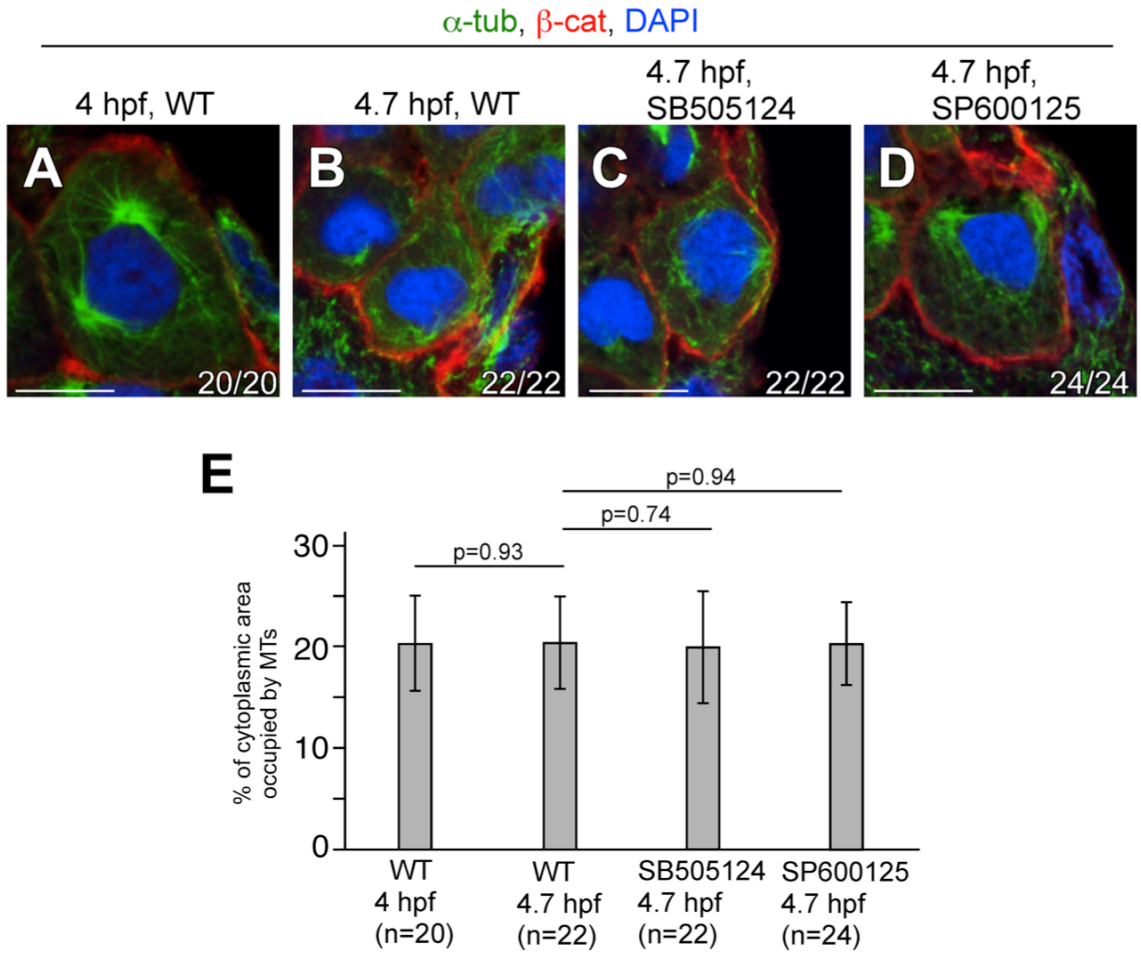

Figure S4. MT formation was not affected by inhibition of Nodal or JNK signaling

(A-D) Cross sections of WT, SB505124-, and SP600125-treated embryos; MTs, cell membrane, and nuclei were visualized by α-tubulin (α-tub), β-cat, and DAPI staining, respectively at 4.0 or 4.7 hpf. Number of nuclei examined is shown at the lower right corner of each panel. Scale bars: 10 μm. (E) Percentage of cytoplasmic area occupied by MTs in LMCs of WT, SB505124-, and SP600125-treated embryos.

Figure S5

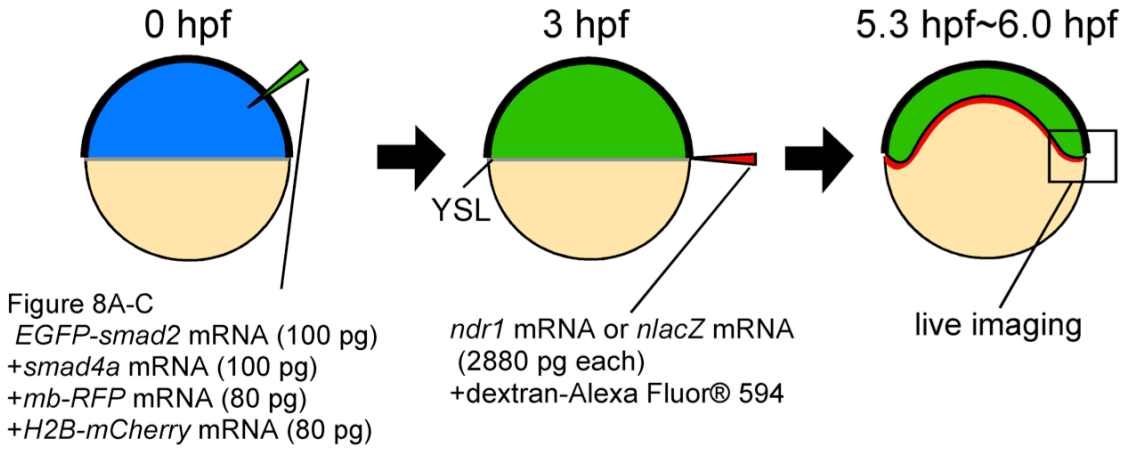

Figure S5. Experimental design of work presented in Figure 8

A mixture of *EGFP-smad2*, *smad4a*, *mb-RFP*, and *H2B-mCherry* mRNAs was injected into WT embryos at the one-cell stage. At 3 hpf, *ndr1* or *nlacZ* mRNA was injected with dextran-Alexa Fluor® 594 into the YSL, and confocal live images were captured at 5.3-6.0 hpf.

Table S1. Primer sequences used for quantitative real-time PCR

Click here to Download Table S1

Movie 1

Time-lapse image of the nucleus in LMC between 4.0 and 4.7 hpf. A white dotted line indicate the boundary between the blastoderm and the YSL. Thick white lines indicate DNBs.

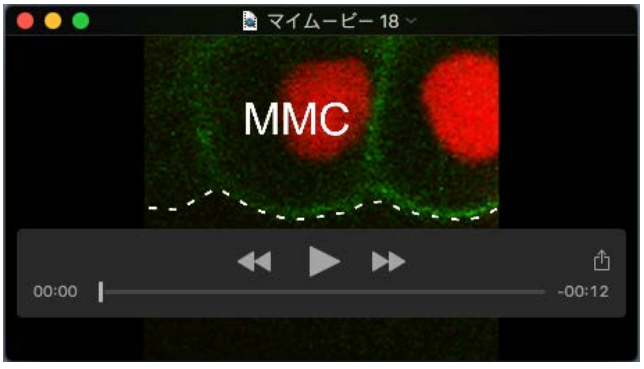

Movie 2

Time-lapse image of the nucleus in MMC between 4.0 and 4.7 hpf. A white dotted line indicate the boundary between the blastoderm and the YSL. Thick white lines indicate DNBs.